

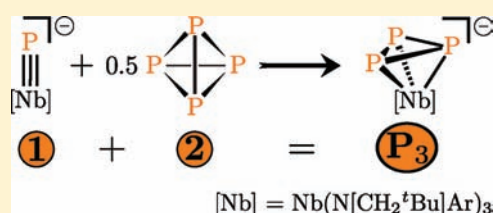
White Phosphorus Activation at a Metal–Phosphorus Triple Bond: a New Route to *cyclo*-Triphosphorus or *cyclo*-Pentaphosphorus Complexes of Niobium

Daniel Tofan, Brandi M. Cossairt, and Christopher C. Cummins*

Department of Chemistry, Massachusetts Institute of Technology, 77 Massachusetts Avenue, Cambridge, Massachusetts 02139, United States

Supporting Information

ABSTRACT: The Nb–P triple bond in $[P\equiv Nb(N[Np]Ar)_3]^-$ ($Np = CH_2^tBu$; $Ar = 3,5-Me_2C_6H_3$) has produced the first case of P_4 activation by a metal–ligand multiple bond. Treatment of P_4 with the sodium salt of the niobium phosphide complex in weakly coordinating solvents led to formation of the *cyclo*- P_3 anion $[(P_3)Nb(N[Np]Ar)_3]^-$. Treatment in tetrahydrofuran (THF) led to the formation of a *cyclo*- P_5 anion $[(Ar[Np]N)(\eta^4-P_5)Nb(N[Np]Ar)_2]^-$, which represents a rare example of a substituted pentaphosphacyclopentadienyl ligand. The P_4 activation pathway was shown to depend on the dimer–monomer equilibrium of the niobium phosphide reagent, which, in turn, depends on the solvent used for the reaction. The pathway leading to the *cyclo*- P_3 product was shown to require a 2:1 ratio of the phosphide anion to P_4 , while the *cyclo*- P_5 formation requires a 1:1 ratio. The *cyclo*- P_3 salt has been isolated in 56% yield as orange crystals of the $[Na(THF)]_2[(P_3)Nb(N[Np]Ar)_3]_2$ dimer or in 83% yield as an orange powder of $[Na(12-crown-4)]_2[(P_3)Nb(N[Np]Ar)_3]$. A solid-state X-ray diffraction experiment on the former salt revealed that each Nb– P_3 unit exhibits pseudo- C_3 symmetry, while ^{31}P NMR spectroscopy showed a sharp signal at -223 ppm that splits into a doublet–triplet pair below -50 °C. It was demonstrated that this salt can serve as a P_3^{3-} source upon treatment with $AsCl_3$, albeit with modest yield of AsP_3 . The *cyclo*- P_5 salt was isolated in 71% yield and structurally characterized from red crystals of $[Na(THF)_6][(Ar[Np]N)(\eta^4-P_5)Nb(N[Np]Ar)_2]$. The anion in this salt can be interpreted as the product of trapping of an intermediate pentaphosphacyclopentadienyl structure through migration of one anilide ligand onto the P_5 ring. The $W(CO)_5$ -capped *cyclo*- P_3 salt was also isolated in 60% yield as $[Na(THF)][(OC)_5W(P_3)Nb(N[Np]Ar)_3]$ from the activation of 0.5 equiv of P_4 with the sodium salt of the tungsten pentacarbonyl adduct of the niobium phosphide anion.



1. INTRODUCTION

Described first by Sacconi et al.,¹ *cyclo*- P_3 ligands have been of interest as products of white phosphorus activation by metal complexes.^{2,3} They have been of interest also as members of an isolobal series of tetrahedra, $P_n\{Co(CO)_3\}_{4-n}$.⁴ Recently, it was shown that *cyclo*- P_3 complexes of niobium and molybdenum could be obtained upon treatment of terminal phosphide ($P\equiv M$) complexes with a source of P_2 ;⁵ in particular, the complex $(\eta^2-PPNMe_s^*)Nb(N[Np]Ar)_3$ ($Ar = 3,5-Me_2C_6H_3$, $Np = CH_2^tBu$, and $Me_s^* = 2,4,6-tBu_3C_6H_2$) serves as a source of P_2 upon thermal fragmentation (Scheme 1).⁶ Spurred by this latter development, we considered the possibility that P_4 itself might be able to serve as a source of two P_2 units upon reaction with a suitable terminal phosphide derivative because this would represent a new and economical “1 + 2” synthesis of *cyclo*- P_3 complexes. For this work, we targeted anionic *cyclo*- P_3 complexes of niobium because these have been employed successfully as P_3^{3-} transfer agents, most notably in the synthesis of AsP_3 .⁷ In the course of detailing a valuable new route to *cyclo*- P_3 complexes, we are also unveiling two unique examples of P_4 activation by a metal–ligand multiple bond, leading to *cyclo*- P_3 and P_5

products. This approach complements the recent application of main-group element systems to the problem of P_4 activation.⁸

2. RESULTS

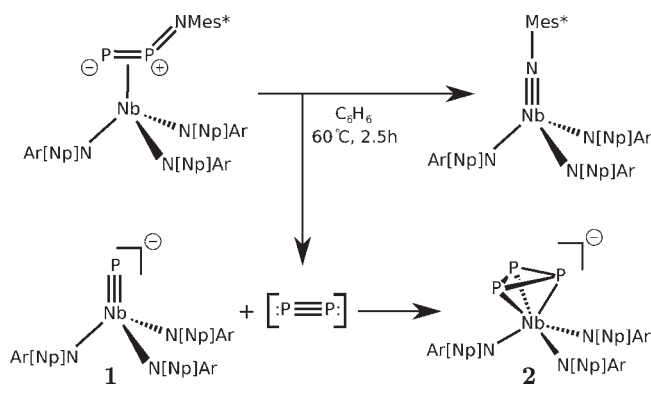
2.1. Synthesis of a *cyclo*- P_3 Salt. Treatment of a benzene solution of phosphide $[Na(OEt_2)]_2[1]_2$ with P_4 led, at room temperature, to a rapid color change from dark yellow to orange (Scheme 2). The product was identified by NMR spectroscopy (both 1H and ^{31}P) as the previously reported $[(\eta^3-P_3)Nb(N[Np]Ar)_3]^-$ anion (2).⁵ The conversion was quantitative by NMR, and using PPh_3 as the internal standard, it was revealed to require only 0.5 equiv of P_4 . Further addition of P_4 does not lead to the appearance of new products. Similar observations were made when using other solvents, including benzene, toluene, diethyl ether, dimethoxyethane, fluorobenzene, benzonitrile, and pyridine.

The product was isolated by recrystallization from pentane solutions containing small amounts of tetrahydrofuran (THF)

Received: July 10, 2011

Published: September 06, 2011

Scheme 1. Previously Reported the Synthesis of Anion 2 from the Trapping of Diposphorus Species by Anion 1⁵



in 56% yield as analytically pure orange crystals of $[\text{Na}(\text{THF})_2][2]_2$. Alternatively, the product can be isolated in 83% yield as the salt $[\text{Na}(12\text{-crown-}4)_2][2]$ after the addition of 2 equiv of 12-crown-4 and isolation of the orange powder from diethyl ether–pentane solutions.

The ³¹P NMR chemical shift of the *cyclo*-P₃ anion 2 was reported in pyridine at –183 ppm when the sodium cation is sequestered by two 12-crown-4 ethers.⁵ In THF and without cation sequestration, the anion appears as a sharp singlet resonance at –223 ppm, this being a significant change in the value of its chemical shift. At low temperatures, in solution, a loss of the 3-fold symmetry of the anion is also observed. The normally sharp ³¹P NMR signal for the anion 2 broadens, and in THF, it splits into two resonances below –50 °C. At –80 °C, it is split into a 2:1 doublet–triplet pair, at –178 and –203 ppm, respectively, with a large one-bond ³¹P–³¹P coupling constant of 250 Hz.

The solid-state structure of the salt of the *cyclo*-P₃ anion was obtained through an X-ray crystallography experiment. This shows that the salt forms a dimer with the formula $[\text{Na}(\text{THF})_2][2]_2$ (Figure 1), reminiscent of the dimeric structure reported for the sodium salt of the phosphide starting material 1.⁹

2.2. Synthesis of a *cyclo*-P₅ Salt. A competing pathway leading to the generation of a new activation product was observed when the treatment of P₄ with anion 1 was carried out in coordinating solvents such as THF. The mixing of THF solutions of P₄ and $[\text{Na}][1]$ at room temperature led to rapid consumption of the phosphide, as the color of the mixture changed from dark yellow to red. Independent of the amount of P₄ used (from 0.25 to over 3 equiv), a different major product formed. This new product has the chemical formula $[\text{Na}(\text{THF})_6][(\text{Ar}[\text{Np}]\text{N})(\eta^4\text{-P}_5)\text{-Nb}(\text{N}[\text{Np}]\text{Ar})_2]$ ($[\text{Na}][3]$) and was also the subject of an X-ray diffraction study (Figure 2). In THF, the formation of the *cyclo*-P₅ anion is quite selective (Scheme 2) because greater than 95% conversion could be recorded by ³¹P NMR spectroscopy by using PPh₃ as an internal standard. This product was isolated in 71% yield as a red-orange solid after recrystallization from pentane–THF mixtures. Minimal competing formation of anion 2 was observed (less than 5%) by ³¹P NMR spectroscopy.

The use of other coordinating solvents for the activation of P₄ led to different ratios of anions 3 and 2 (Table 1). Upon switching to THF derivatives with increased steric hindrance around the oxygen atom such as 2-methyltetrahydrofuran and 2,5-dimethyltetrahydrofuran, the ratio of anion 3 to 2 produced

under the same conditions decreases from 10:1 to 9:1 and 6.4:1, respectively (by ³¹P NMR). Using 1,4-dioxane as a solvent decreased the ratio to 3.7:1. The formation of both 3 and 2 was observed when the reaction was performed in acetonitrile, in a 4.5:1 ratio. In addition, small amounts of the anion 3 could also be observed when using diethyl ether if stoichiometric amounts of THF were present, such as when $[\text{Na}(\text{THF})_x][1]$ ($x = 2\text{--}3$) was employed as the phosphide source. The use of other polar, coordinating solvents such as dimethoxyethane, pyridine, fluoro-benzene, benzonitrile, or dichloromethane did not lead to products other than the *cyclo*-P₃ anion 2 (by ³¹P NMR spectroscopy).

The room temperature ³¹P NMR spectrum of the isolated anion 3 contains five distinct peaks, with one of these resonating as a triplet at +78 ppm in THF. The remaining four signals resonate between –10 and –100 ppm but are very broad. Below –40 °C, these signals sharpen into well-resolved pseudotriplets at –5, –40, –59, and –87 ppm, respectively. Spectrum fitting using the *g*NMR software package¹¹ revealed some large P–P one-bond coupling constants between 330 and 405 Hz, as well as appreciable two-bond coupling constants of +27 and –34 Hz (Figure 3).

2.3. Related Activations. Treatment of the capped phosphide $[\text{Na}(\text{OEt}_2)][(\text{OC})_5\text{WPb}(\text{N}[\text{Np}]\text{Ar})_3]$ ($[\text{Na}][1\text{-W}]$) with P₄ in nonpolar solvents led to reactivity similar to that observed for 1. A very broad singlet at –219 ppm was recorded in the ³¹P NMR spectrum, characteristic for the previously reported anion $[(\text{OC})_5\text{W}(\text{P}_3)\text{Nb}(\text{N}[\text{Np}]\text{Ar})_3]^-$ (2-W).⁵ This complex was isolated in 60% yield as an orange powder after recrystallization from pentane–THF mixtures, as the $[\text{Na}(\text{THF})][2\text{-W}]$ salt. Unlike with the phosphide 1, treatment in THF of the capped phosphide 1-W with P₄ did not generate new products because only the anion 2-W could be observed by NMR spectroscopy.

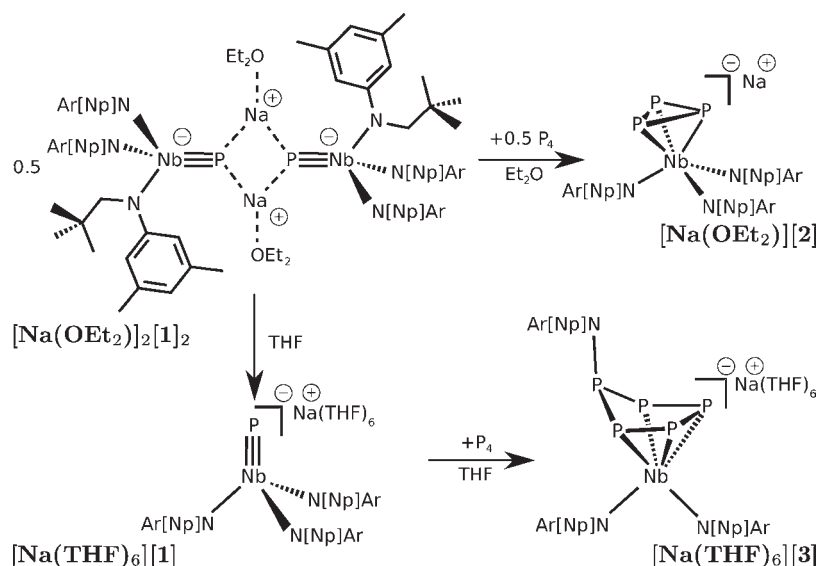
On the other hand, no reaction was observed upon treatment of the neutral (trimethylsilyl)phosphinidene complex $\text{Me}_3\text{SiP}=\text{Nb}(\text{N}[\text{Np}]\text{Ar})_3$ ⁹ with P₄. Treatment of the related arsenide $[\text{Na}][\text{As}=\text{Nb}(\text{N}[\text{Np}]\text{Ar})_3]$ ¹² with 1 equiv of P₄ in diethyl ether led to the appearance of new peaks in the ³¹P NMR spectrum. These can be attributed to the expected *cyclo*-AsP₂ niobium complex, as well as to *cyclo*-P₃ and *cyclo*-As₂P products. A similar product distribution (together with small amounts of P₄) was observed when equimolar amounts of AsP₃⁷ and phosphide 1 were mixed together in diethyl ether (Figure 4).

The activation of AsP₃ by the phosphide 1 in THF leads to reactivity similar to that observed for P₄. The formation of multiple isomers of the expected *cyclo*-AsP₄ product was observed by ³¹P NMR spectroscopy. Four different isomers can be identified by low-temperature ³¹P NMR spectroscopy if the analysis is done promptly after mixing. Two of these isomers persist after 1 day in solution at room temperature.

The activation of P₄ molecules was also attempted using $[\text{Na}(12\text{-crown-}4)_2][1]$ as the phosphide source.⁹ When either THF or diethyl ether was used as the solvent for the reaction, essentially selective conversion to the $\eta^4\text{-P}_5$ anion 3 was observed to occur by ³¹P NMR spectroscopy.

3. DISCUSSION

3.1. Structure of the *cyclo*-P₃ Salt. The *cyclo*-P₃ dimer $[\text{Na}(\text{THF})_2][2]_2$ has a Na₂P₂ diamond core. There are four significant Na–P interactions for each of the sodium ions ranging from 2.9792(9) to 3.0961(9) Å. In the solid state, the Nb–P distances are observed at 2.5272(5), 2.5447(5), and 2.5456(5) Å.

Scheme 2. Reactivity Channels for P₄ Activation^a

^a Distinct pathways are followed when the phosphide anion salt is dimeric (top) or monomeric (bottom).

The three P–P bonds are very close in distance, coming at 2.1724(7), 2.1745(7), and 2.1749(7) Å. Even though in the solid state only one of the three phosphorus atoms of anion **2** interacts with two sodium cations, the {P₃Nb} tetrahedron is still close to being 3-fold symmetric. In addition to the four Na–P interactions and the one with the THF ligand, the coordination sphere of each sodium ion is completed through a cation– π interaction with three aryl carbon atoms from one anilide ligand.

This pseudo-C₃ symmetry of anion **2** leads to a single anilide and a single phosphorus environment at room temperature by solution NMR spectroscopy. However, not having the cation sequestered by crown ethers leads to an apparent decrease in the 3-fold symmetry in solution at low temperatures. The normally sharp ³¹P NMR signal for the anion **2** splits into two resonances at low temperatures, indicative of an ion-pairing interaction that desymmetrizes the *cyclo*-P₃ ring. These observations suggest that the dimer is conserved in solution, even in THF, which is different from the behavior of the phosphide anion **1**. At room temperature this dimer undergoes a fast scrambling of the P–Na interactions, probably through a $\mu, \eta^{1:3} \rightleftharpoons \mu, \eta^{3:1}$ exchange, which, at cryogenic temperatures, becomes frozen out.

Given the reactivity of the related [(P₃)Nb(ODipp)₃][−] anion,⁷ the anion **2** was also targeted as a P₃^{3−} transfer agent. Under the same conditions as those reported in the literature,⁷ the treatment of the anion **2** with AsCl₃ did lead to the formation of AsP₃. However, unlike the 70% isolated yield reported when using [(P₃)Nb(ODipp)₃][−], the observed spectroscopic yield of AsP₃ from the anion **2** was only approximately 14%. This provides a clear demonstration that the AsP₃-forming reaction is sensitive to the nature of the ancillary ligands.

3.2. Structure of the *cyclo*-P₅ Salt. There are two crystallographically distinct but chemically equivalent molecules of [Na(THF)₆][**3**] in the asymmetric unit obtained from X-ray diffraction experiments. The five phosphorus atoms form a five-membered ring, and in one of the two conformations (depicted in Figure 2), the P–P bond distances range from 2.1550(18) to 2.1894(19) Å, close to the average value for P–P single bonds of 2.21 Å.¹³ Four of the phosphorus atoms bind to niobium, while

the fifth one binds to an anilide group. The η^4 -bonding to niobium includes a relatively long contact at 2.6968(14) Å, two medium ones at 2.5961(14) and 2.6151(13) Å, and a shorter one at 2.5380(14) Å. These values are in the range of Nb–P single bonds because even the shortest of them is significantly longer than the reported values for Nb–P double bonds.^{9,13,14} The metal coordination sphere is completed by an additional set of two metal–aryl interactions from the niobium-bound anilide ligands. In both the ¹H and ¹³C NMR spectra, the complex exhibits C₁ symmetry at room temperature, with three distinct anilide environments, consistent with the observed solid-state structure of the anion.

The structure of anion **3** suggests a [RP₅]^{4−} formulation for the *cyclo*-P₅ ligand, which has cyclopentaphosphane, P₅H₅, as a parent molecule.¹⁵ The η^4 -coordination, together with the two nitrogen atoms, is not enough to satisfy the coordination sphere of niobium; this is fulfilled with a pair of metal–aryl interactions. This type of η^3 binding mode by the anilide ligands has been observed in several other instances when the metal center is electron-deficient, including in the case of Ti(NR_{Ar})₃ and V(NR_{Ar})₃.¹⁶ Also, this is very similar to the η^3 binding mode for benzyl ligands as originally described by Cotton and LaPrade.¹⁷ The metal–aryl interactions observed here of just over 2.5 Å in the solid state are too long to be described as Nb–C single bonds, which are typically below 2.3 Å.¹³ However, they are sufficiently strong to prevent free rotation around the metal–nitrogen bond in solution. Therefore, the pseudo-C₂ symmetry of the rigid {Nb(N[Np]Ar)₂} fragment combined with mirror symmetry for the {Ar[Np]N(P₅)} ligand leads to the C₁ symmetry observed for the anion **3** by NMR spectroscopy at room temperature, with five phosphorus and three distinct anilide environments.

The only previously reported early-transition-metal complex bearing a cyclopentaphosphane ligand is the [Ti(P₅)₂]^{2−} anion.^{3,18} To our knowledge, the anion **3** is the first example of a monometallic structure where a substituted cyclopentaphosphane {RP₅} ligand is η^4 -bound to a metal. There are only a few multimetallic late-transition-metal complexes that exhibit a similar binding

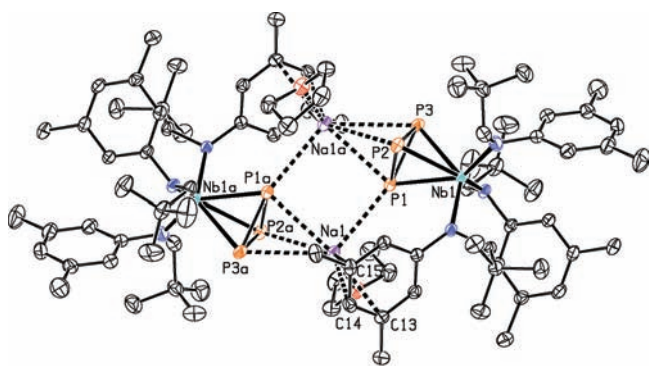


Figure 1. Solid-state structure of the $[\text{Na}(\text{THF})_2]_2[2]_2$ dimer rendered in PLATON¹⁰ with ellipsoids at the 50% probability level and hydrogen atoms omitted for clarity. Selected distances [Å] and angles [deg]: Nb1–P1 2.5447(5), Nb1–P2 2.5272(5), Nb1–P3 2.5456(5), P1–P2 2.1749(7), P1–P3 2.1745(7), P2–P3 2.1724(7), Na1–P1 2.9812(9), Na1–P1a 2.9792(9), Na1–P2a 3.0708(9), Na1–P3a 3.0961(9), Na1–C13 2.9793(19), Na1–C14 2.7828(19), Na1–C15 2.8513(19), Nb1–N1 2.0427(15), Nb1–N2 2.0526(15), Nb1–N3 2.0762(16); P1–Na1–P1a 87.16(2), Na1–P1–Na1a 92.84(2), Nb1–P1–Na1 129.56(2), Nb1–P1–Na1a 128.73(2), P3–P1–P2 59.93(2), P1–P2–P3 60.03(2), P2–P3–P1 60.04(2).

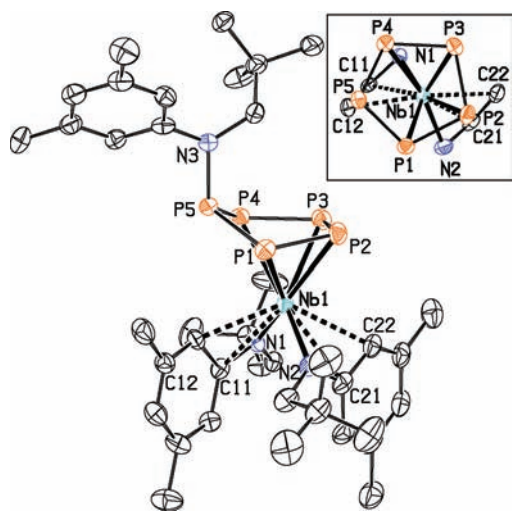


Figure 2. Solid-state structure of the $[\text{Na}(\text{THF})_6]_3[3]$ salt rendered in PLATON¹⁰ with ellipsoids at the 50% probability level. Hydrogen atoms and the $[\text{Na}(\text{THF})_6]^+$ cation are omitted for clarity. The coordination environment around the metal in anion 3 is shown in the top-right inset as a cropped view from above the P_5 ring. Selected distances [Å] and angles [deg]: Nb1–P3 2.5380(14), Nb1–P2 2.5961(14), Nb1–P1 2.6151(13), Nb1–P4 2.6968(14), Nb1–P5 3.3898(14), P1–P2 2.160(2), P2–P3 2.1894(19), P3–P4 2.1622(18), P4–P5 2.1550(18), Nb1–C11 2.605(5), Nb1–C12 2.535(5), Nb1–C21 2.597(5), Nb1–C22 2.606(5), Nb1–N1 2.091(4), Nb1–N2 2.093(4), P5–N3 1.751(4); P5–P1–P2 106.30(8), P1–P2–P3 105.80(7), P2–P3–P4 103.02(7), P3–P4–P5 110.67(7), P4–P5–P1 98.10(7).

motif, the most similar of which is the bimetallic complex $[\{\text{Cp}^*(\text{OC})_2\text{Fe}\}(\mu, \eta^{1:4}\text{-P}_5\text{Me})\{\text{FeCp}^*\}]$, which was isolated as a reaction byproduct in low yield.¹⁹ Other examples of P_5 units bound to a metal in an η^4 fashion include the trimetallic complex $[\{\text{Cp}^*(\text{OC})\text{Ir}\}_2(\mu^3, \eta^{1:1:4}\text{-P}_5)\{\text{FeCp}^*\}]$,²⁰ and a few examples where a P_{10} unit, comprised of two P_5 cycles joined by a P–P

Table 1. Solvent versus Product Distribution

solvent ^a	ratio of anions 3 to 2 ^b
pentane	0
2,3-dimethylbutadiene	0
dioxane	3.7
benzene	0
toluene	0
1,3-cyclohexadiene	0
diethyl ether	0
fluorobenzene	0
2,5-dimethyltetrahydrofuran	6.4
2-methyltetrahydrofuran	9
dimethoxyethane	0
tetrahydrofuran	10
dichloromethane	0 ^c
pyridine	0
benzonitrile	0
acetonitrile	4.5

^a Experimental conditions: phosphide 1 and excess solid P_4 (2.7 equiv) stirred for 1 h. ^b Recorded by ³¹P NMR spectroscopy. ^c In dichloromethane, the *cyclo*- P_3 product reacts further with the solvent.

bond, are η^4 -bound to multiple metals.²¹ Activations of P_4 resulting in η^4 -bound phosphorus fragments in transition-metal complexes are also known.²²

3.3. Activation of P_4 with Niobium Phosphides. In non-polar solvents, the activation of P_4 molecules, with either the uncapped phosphide anion 1 or the $\text{W}(\text{CO})_5$ -capped one (1-W), leads to *cyclo*- P_3 products. The phosphide anions undergo a formal addition of P_2 units to the metal–phosphorus multiple bonds to form the *cyclo*- P_3 complexes. $[\text{Na}(12\text{-crown-4})_2][2]$ and $[\text{Na}(12\text{-crown-4})_2][2\text{-W}]$ had been isolated previously from the trapping of P_2 or $(\text{P}_2)\text{W}(\text{CO})_5$ by the phosphide 1 in yields of 30% and 75%, respectively (Scheme 1).⁵ The yields obtained here, 56% for anion 2 and 60% for anion 2-W, are on par with those obtained previously for the *cyclo*- P_3 anions. However, the approach reported here represents a simpler, synthetically useful methodology for the synthesis of salts of the *cyclo*- P_3 anion because the source of P_2 units is elemental phosphorus, rather than the complicated niobium diphosphaazide complex used previously, which itself is the product of a multistep synthesis originating from P_4 .⁵ In addition, the method disclosed here also removes the requirement to sequester the cation with crown ethers for purposes of product separation.

A lack of reactivity between the neutral (trimethylsilyl)-phosphinidene complex $\text{Me}_3\text{SiP}=\text{Nb}(\text{N}[\text{Np}]\text{Ar})_3$ and P_4 is observed. This indicates that the presence of the ionic charge may be a requirement for the activation of P_4 molecules by metal–phosphorus multiple bonds. Treatment of diethyl ether solutions of the related arsenide $[\text{Na}][\text{As}=\text{Nb}(\text{N}[\text{Np}]\text{Ar})_3]$ with P_4 , or of the phosphide 1 with AsP_3 , led to observations consistent with the facile scrambling of pnictogen atoms (Figure 4). Such a distribution of *cyclo*- $\text{As}_x\text{P}_{3-x}$ products has been reported for a related niobium system.²³ The scrambling takes place in the course of the formation of *cyclo*- E_3 ligands and not subsequently, as the scrambling between the *cyclo*- P_3 product and unreacted AsP_3 has been ruled out in a control experiment.

A different product distribution was observed when coordinating solvents were employed for the activation of P_4 by phosphide 1 (see Table 1). Specifically, when THF was employed,

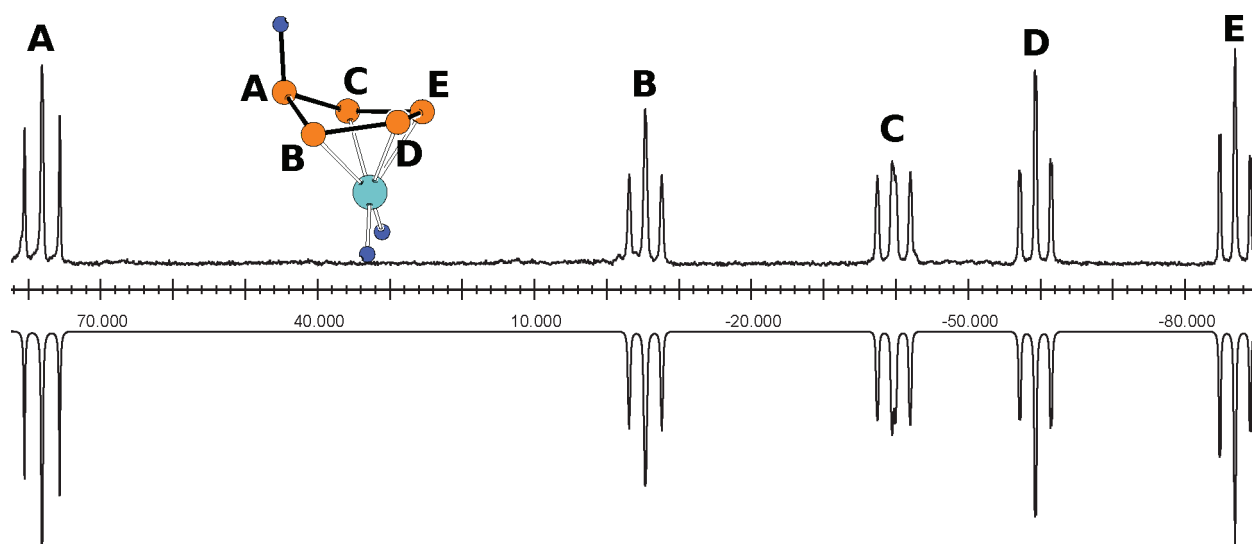


Figure 3. ^{31}P NMR spectrum of anion **3** (in THF, $-80\text{ }^\circ\text{C}$, 162 MHz) showing experimental (top) and fitted (bottom) spectra.¹¹ Coupling constants (Hz) obtained from the fit: $^1J_{ab} = 383$, $^1J_{ac} = 405$, $^1J_{bd} = 350$, $^1J_{ce} = 330$, $^1J_{de} = 351$, $^2J_{ad} = -4.8$, $^2J_{be} = 27$, and $^2J_{cd} = -34$.

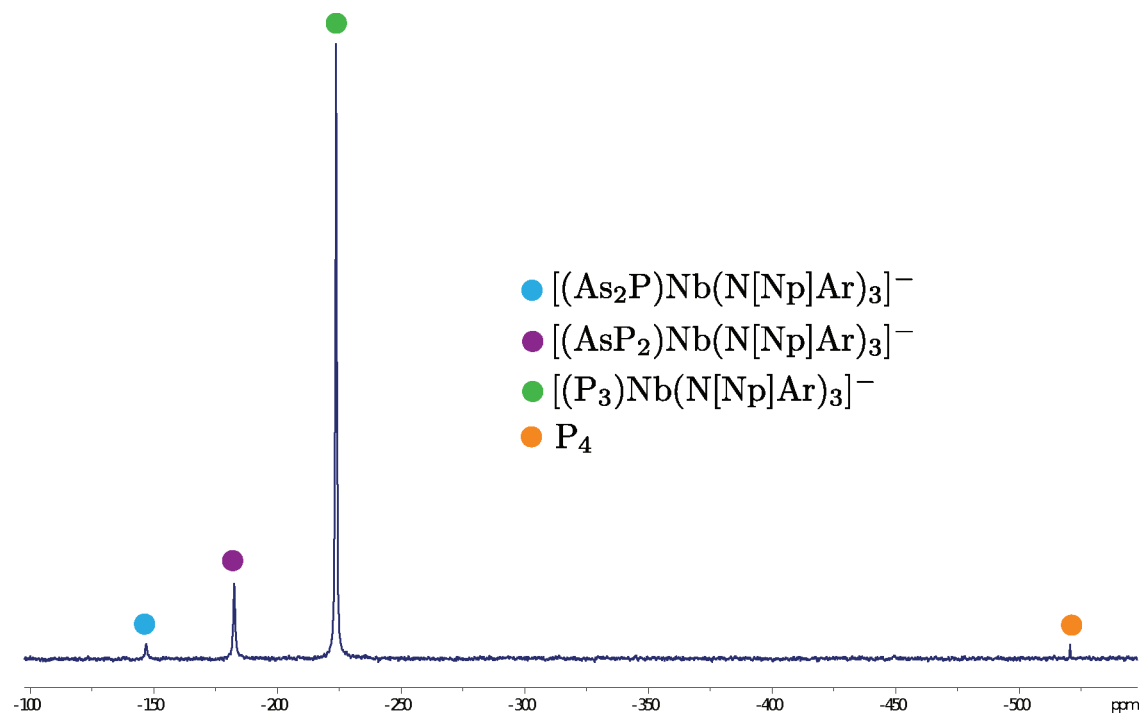


Figure 4. ^{31}P NMR spectrum obtained 20 min after the activation of AsP_3 with the niobium phosphide anion **1** in a diethyl ether solution. Scrambling of pnictogen atoms produces the anion **2** as the major product, with the *cyclo*- AsP_2 and As_2P anions as well as a small amount of P_4 forming in smaller quantities.

a conversion to the *cyclo*- P_5 product of over 90% was observed. Instead of a molecule of P_4 being split by two phosphide anions, a whole molecule is consumed by a single phosphide. The phosphide anion essentially undergoes a formal addition of an entire P_4 molecule to form the novel *cyclo*- P_5 anion **3**. This result can be interpreted as the trapping of an intermediate pentaphosphacyclopentadienyl structure through the migration of one of the anilide ligands from the metal center onto a phosphorus atom.

The conversion becomes less selective for the formation of anion **3** as the solvent is replaced with THF derivatives. The

dielectric constant does not change significantly upon moving from THF to 2-methyltetrahydrofuran and 2,5-dimethyltetrahydrofuran, decreasing from 7.52 to 6.97 and ~ 6 , respectively.²⁴ On the other hand, the decrease in selectivity is paralleled by an increased steric hindrance about the oxygen atom of the solvent molecules. Neither pyridine nor benzonitrile, which have large dielectric constants of 12.26 and 25.9, respectively, shows any selectivity for the *cyclo*- P_5 product when used as a solvent.

The solid-state structure of the niobium phosphide sodium salt, which was used for the activation of P_4 , was reported previously

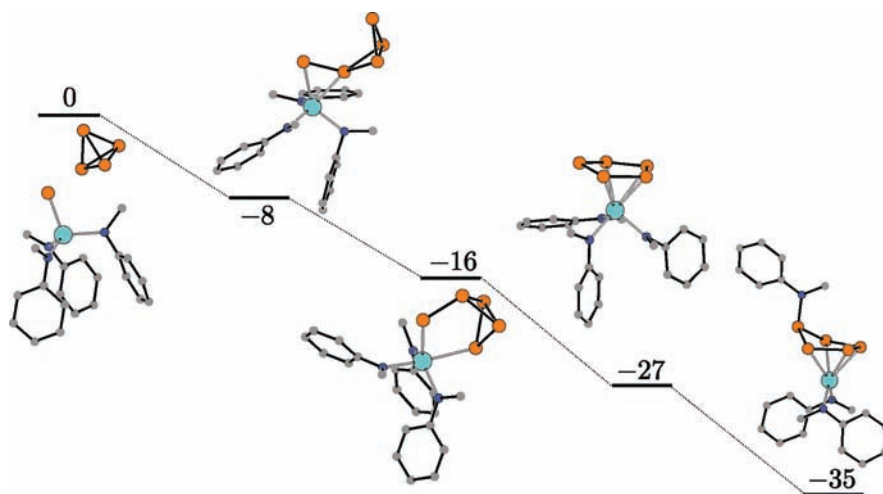


Figure 5. Computed energy diagram (in kcal/mol) for the activation of P_4 by the model phosphide anion $[P\equiv Nb(N[Me]Ph)_3]^-$. Several possible intermediate structures are also shown, and their electronic energies are referenced against the sum of the energies for a molecule of P_4 and a phosphide anion.²⁹

using crystals obtained from ethereal solutions. This sodium salt of **1** exists as a dimer, with the molecular formula $[Na(OEt_2)]_2[1]_2$.⁹ This dimeric form is preserved in weakly coordinating solvents, but in THF, it is broken apart as the cation is sequestered away by solvent molecules. This interpretation is corroborated by a significant downshift in the ^{31}P NMR chemical shift of the phosphide ^{31}P nucleus upon going from benzene to THF.⁹ Because the formation of anion **3** became disfavored with respect to that of **2** in solvents having lower affinity for the sodium ion, we postulate that the appearance of P_5 structures requires the breaking apart of the dimer of phosphide **1**. Literature precedent exists for the reactivity influence of an ethereal solvent through a shift in the dimer \rightleftharpoons monomer equilibrium, including for alkali-metal salts.²⁵ This hypothesis was verified by using $[Na(12\text{-crown-4})_2][1]$ as the phosphide source, in which it has been shown that the sodium cation is sequestered by crown ethers, while the anion is in a “naked”, monomeric form.⁹ Indeed, even when using diethyl ether as the solvent, essentially selective conversion to the $\eta^4\text{-}P_5$ anion **3** was observed.

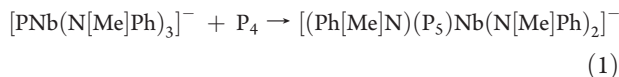
In nonpolar solvents, we postulate that a dimeric phosphide $[Na(OEt_2)]_2[P\equiv Nb(N[Np]Ar)_3]_2$ molecule reacts directly with P_4 and breaks it into halves to generate two niobium *cyclo*- P_3 anions. Because the product is believed to be dimeric in solution, it is possible that this pathway does not involve the breaking of the Na_2P_2 diamond core at any point during the reaction. However, because phosphide anions **1** are capable of trapping diphosphorus species to yield the *cyclo*- P_3 anions **2**,⁵ an alternative pathway can also be envisioned: a monomeric phosphide anion **1** may react with a P_4 molecule to form the anion **2** with the release of P_2 , which is later, in turn, trapped by a second phosphide molecule. In order to probe for the possible intermediacy of P_2 in the process leading to *cyclo*- P_3 complexes, the P_4 activation reaction was performed in neat 1,3-cyclohexadiene and in neat 2,3-dimethylbutadiene and monitored for the formation of new products. Although anion **2** was observed in each case, none of the expected trapping products could be detected using either 1,3-cyclohexadiene⁶ or 2,3-dimethylbutadiene.²⁶ It remains a possibility that the dienes were unable to compete with the phosphide anion **1** for the trapping of any P_2 that may have been generated.

The activation of P_4 molecules with the related $W(CO)_5$ -capped phosphide $[Na(OEt_2)][(OC)_5WPb(N[Np]Ar)_3]$ (**1-W**) in THF led to the formation of only the $[Na(THF)][(OC)_5W(P_3)Nb(N[Np]Ar)_3]$ (**2-W**) product. The reported solid-state structure of the capped phosphide **1-W** indicated a monomeric constitution.⁵ It is possible that one anion **1-W** reacts with P_4 to generate the *cyclo*- P_3 anion **2** together with $(\eta^2\text{-}P_2)W(CO)_5$.²⁷ The trapping of the latter entity with another **1-W** anion, followed by the scrambling of $W(CO)_5$ units would yield **2-W** as a net product. However, attempts to intercept $(\eta^2\text{-}P_2)W(CO)_5$ species by carrying out the reaction in 2,3-dimethylbutadiene did not lead to any 1H or ^{31}P NMR resonances corresponding to those of the reported diene-trapping product $(OC)_5WP_2C_{12}H_{20}$.⁶

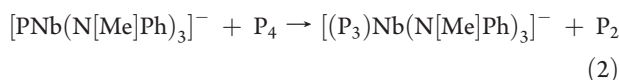
The activation of AsP_3 by phosphide **1** in THF leads to both *cyclo*- AsP_3 and *cyclo*- AsP_4 products. Low-temperature ^{31}P NMR spectroscopy allowed for the identification of four different isomers of the expected *cyclo*- AsP_4 unit, each with the arsenic atom bound to niobium. However, two of these isomers do not appear to be stable at room temperature in solution for extended periods of time.

3.4. Computational Insights on the Activation of P_4 . Using density functional theory (DFT),²⁸ we investigated the energetics of the reaction of the “naked” phosphide monomer with P_4 using the simplified model $[P\equiv Nb(N[Me]Ph)_3]^-$. Geometries were optimized in a continuum dielectric model for THF, leading to viable intermediate structures en route to the formation of anion $[(Ph[Me]N)(P_3)Nb(N[Me]Ph)_2]^-$ (Figure 5).²⁹ An η^2 -bound phosphinophosphinidene complex $[P=PR_2, \text{ for } R_2 = (P_3)]^-$ was found to be at -8 kcal/mol with respect to the starting molecules (electronic energy). This anion can be envisioned as the product of the insertion of a vertex of P_4 into the Nb–P triple bond and is reminiscent of some previously reported phosphinophosphinidene complexes of niobium $[(\eta^2\text{-}R_2PP)Nb(N[Np]Ar)_3]$ ($R = t\text{-Bu, Ph}$).⁹ A $\kappa^2\text{-}P_5$ structure, which can be envisioned as the insertion of one of the edges of the P_4 tetrahedron into the phosphide multiple bond, was found to be another 8 kcal/mol more stable. Another structure with a planar cyclopentaphosphane ring η^4 -bound to niobium was found to be quite stable, at -27 kcal/mol from the starting materials. If this intermediate does form, the phosphorus atom not bound to niobium is poised

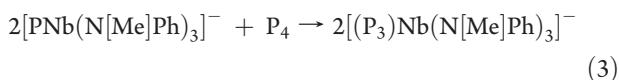
to undergo anilide transfer from the metal center, to generate the observed final product. The overall transformation that follows (eq 1) was predicted to ensue with a release of 35 kcal/mol of energy.



It is unclear how the *cyclo*-P₃ anion **2** is produced from the monomeric phosphide **1**, such as is observed when using [Na(12-crown-4)₂][**2**]. It is possible that a P₂ molecule is extruded from one of the intermediates. We investigated the transformation that follows (eq 2) with DFT and found the products to be less than 1 kcal/mol above the energy level of the reactants.



It is also possible that some intermediate structures are sufficiently long-lived to allow for a bimolecular reaction with another phosphide to yield two *cyclo*-P₃ anions. This pathway should be preferred when excess phosphide **1** is present. The overall reaction of two phosphide anions and one P₄ molecule (eq 3) was predicted to be energetically downhill by 51 kcal/mol.



4. CONCLUSION

We have been able to show for the first time how a metal–ligand multiple bond can be employed to activate P₄ molecules and how the activation mechanism is dependent upon the solvent choice. The use of weakly coordinating solvents provides streamlined access to the anionic *cyclo*-P₃ niobium anions **2** and **2-W** in high yield without any need for crown ethers in their isolation. The potential utility of anion **2** as a P₃³⁻ transfer agent can now be investigated. The use of THF as a solvent for the activation of P₄ provides selective access to the *cyclo*-P₅ niobium anion **3** following the Nb → P transfer of an anilide group. Anion **3** exhibits an unusual binding motif among P₅ ligands and represents a rare example of controlled building of P_{4+n} assemblies from P₄ and a P_n source.

5. EXPERIMENTAL SECTION

5.1. General Procedures. All manipulations were performed in a Vacuum Atmospheres model MO-40M glovebox under an inert atmosphere of purified N₂. Dioxane was distilled from sodium benzophenone and pyridine from CaH₂, while 2-methyltetrahydrofuran and 2,5-dimethyltetrahydrofuran were degassed and dried over sieves for several months. All other solvents were obtained anhydrous and oxygen-free by bubble-degassing (N₂) and purification using a Glass Contours Solvent Purification System built by SG Water. Benzene-*d*₆ was purchased from Cambridge Isotope Laboratories, degassed, and stored over molecular sieves for at least 2 days prior to use. All glassware was oven-dried at temperatures greater than 170 °C prior to use. ¹H, ¹³C, and ³¹P NMR spectra were obtained on a Varian Mercury 300 or a Bruker Avance 400 instrument equipped with Oxford Instruments superconducting magnets and were referenced to residual C₆D₆ signals (¹H, 7.16 ppm; ¹³C, 128.39 ppm). ³¹P NMR spectra were referenced externally to 85% H₃PO₄ (0 ppm). Elemental analyses were performed by Midwest Microlab LLC, Indianapolis, IN. White phosphorus was acquired from Thermphos International. Compounds AsP₃,⁷ [Na(OEt₂)₂][P≡Nb(N[Np]Ar)₃]₂,⁹

[Na(OEt₂)][{(OC)₅WP≡Nb(N[Np]Ar)₃}]⁶ and [Na(OEt₂)][As≡Nb(N[Np]Ar)₃]¹² were prepared according to literature protocols. Partial spectroscopic characterization of anions [(η³-P₃)Nb(N[Np]Ar)₃]⁻ and [(OC)₅W(P₃)Nb(N[Np]Ar)₃]⁻ was reported previously.⁵

5.2. [Na(OEt₂)₂](η³-P₃)Nb(N[Np]Ar)₃]₂ ([Na][2**]).** [Na(OEt₂)₂][**1**]₂ (850 mg, 0.54 mmol, 1.0 equiv) was dissolved in 20 mL of toluene and was combined with a P₄ (67 mg, 0.54 mmol, 1.0 equiv) solution in 5 mL of toluene. The reaction mixture was allowed to stir for 30 min, after which it was concentrated under reduced pressure to a total of 5 mL. After the addition of a few drops of THF, crystallization at -35 °C yielded bright-orange crystals. Further batches were obtained from hexane at -35 °C, resulting in a total of 510 mg (0.30 mmol, 56% yield) of analytically pure [Na(THF)₂](P₃)-Nb(N[Np]Ar)₃]₂. ¹H NMR (C₆D₆, 20 °C, 400 MHz): δ 0.993 (s, 54 H, ^tBu), 1.444 (s, 8 H, THF), 2.278 (s, 36 H, ArCH₃), 3.618 (s, 8 H, THF), 3.945 (s, 12 H, NCH₂), 6.548 (s, 6 H, *p*-Ar), 6.944 (s, 12 H, *o*-Ar). ³¹P{¹H} NMR (C₆D₆, 20 °C, 161.9 MHz): δ -224 (s, 3 P). ³¹P{¹H} NMR (THF, -90 °C, 202 MHz): δ -178 (d, 2 P, ¹J_{PP} = 250 Hz), -203 (t, 1 P). Elem anal. Calcd for C₆₆H₁₃₆N₆Na₂Nb₂O₂P₆: C, 60.63; H, 8.05; N, 4.93; P, 10.91. Found: C, 60.55; H, 8.09; N, 4.90; P, 11.09.

5.3. [Na(C₈H₁₆O₄)₂](P₃)Nb(N[Np]Ar)₃]. [Na(OEt₂)₂][**1**]₂ (505 mg, 0.32 mmol) was dissolved in 10 mL of diethyl ether and was combined with a P₄ (41 mg, 0.33 mmol, 1.0 equiv) solution in 3 mL of toluene. The reaction mixture was allowed to stir for 30 min, after which it was filtered through a glass paper plug and concentrated under reduced pressure to a total of 5 mL. After the addition of 12-crown-4 (223 mg, 1.26 mmol, 4.0 equiv) in 3 mL of diethyl ether, the reaction mixture was stirred for another 15 min, then layered with 5 mL of pentane, and stored at -35 °C. The resulting orange powder was collected on a sintered glass frit, washed with pentane, and dried in vacuo. The solvent was removed from the filtrate in vacuo, and further material was obtained by washing the resulting residue with pentane, yielding [Na(12-crown-4)₂](P₃)Nb(N[Np]Ar)₃] as a bright-orange powder (599 mg, 0.59 mmol, 83% yield).

5.4. [Na(THF)][(OC)₅W(P₃)Nb(N[Np]Ar)₃] ([Na][2-W**]).** [Na(OEt₂)][**1-W**] (749 mg, 0.67 mmol) was dissolved in 20 mL of toluene and was combined with a P₄ (42 mg, 0.34 mmol, 0.5 equiv) solution in 5 mL of toluene. The reaction mixture was allowed to stir for 30 min, after which time the reaction mixture was filtered, dried under reduced pressure, and redissolved in hexane. Storage of this hexane solution at -35 °C yielded an ochre powder. This and further batches were collected by filtration, resulting in a total of 472 mg (0.41 mmol, 60% yield) of pure [Na(THF)][(OC)₅W(P₃)Nb(N[Np]Ar)₃]. ¹H NMR (C₆D₆, 20 °C, 400 MHz): δ 1.121 (s, 27 H, ^tBu), 1.373 (s, 4 H, THF), 2.120 (s, 18 H, ArCH₃), 3.476 (s, 4 H, THF), 4.089 (s, 6 H, NCH₂), 6.407 (s, 3 H, *p*-Ar), 6.842 (s, 6 H, *o*-Ar). ³¹P NMR (Et₂O, 20 °C, 161.9 MHz): δ -219 (vbr s, 3 P).

5.5. [Na(THF)_x](Ar[Np]N){η⁴-P₅}Nb(N[Np]Ar)₂] ([Na][3**]).** [Na(OEt₂)₂][**1**]₂ (703 mg, 0.45 mmol) was dissolved in 10 mL of THF. Solid P₄ (114.0 mg, 0.92 mmol, 2.0 equiv) was added to the stirring solution at 20 °C, and the color of the solution immediately changed from dark orange to dark red. After stirring for 1 h, the mixture was concentrated to ca. half of the volume. Pentane (ca. 5 mL) was added and the mixture stored at -35 °C to yield bright, orange solids that were collected in several crops, resulting in a total of 762 mg (>71% yield) of pure [Na(THF)_{x>6}](Ar[Np]N){μ,η^{1:4}-P₅}Nb(N[Np]Ar)₂]. ¹H NMR (C₆D₆, 20 °C, 500 MHz): δ 7.33 (s, 2 H, *o*-Ar), 7.27 (s, 2 H, *o*-Ar), 7.20 (s, 2 H, *o*-Ar), 6.59 (s, 1 H, *p*-Ar), 6.54 (s, 1 H, *p*-Ar), 6.50 (s, 1 H, *p*-Ar), 4.34 (s, 2 H, CH₂^{Nb}), 4.32 (s, 2 H, CH₂^{Nb}), 3.74 (bs, 14 Hz, 2H, CH₂^P), 2.40 (s, 6 H, Ar-CH₃), 2.24 (s, 6 H, Ar-CH₃), 2.22 (s, 6 H, Ar-CH₃), 1.08 (s, 9 H, ^tBu), 1.02 (s, 9 H, ^tBu), 1.00 (s, 9 H, ^tBu). ³¹P{¹H} NMR (C₆D₆, 20 °C, 121.5 MHz): δ +82.2 (t, 1 P, N-P^a, ¹J_{PP} = 377 Hz), -28.9 (vbr, 1 P, P^b), -42.5 (vbr, 1 P, P^c), -77.2 (vbr, 1 P, P^d), -115.8 (vbr, 1 P, P^e). ³¹P{¹H} NMR (THF, -80, 161.9 MHz): δ +78.1 (t, N-P^a, ¹J_{ab} = 383 Hz, ¹J_{ac} = 405 Hz, ²J_{ad} = -4.8 Hz), -5.4 (t, P^b, ¹J_{bd} = 350 Hz, ²J_{be} = 27 Hz), -39.7 (dd, P^c, ¹J_{ce} = 330 Hz,

Table 2. Crystallographic Data for Salts of 2 and 3

	[Na(THF)] ₂ [2] ₂	[Na(THF) ₆][3]
Reciprocal Net code/CCDC number	11074/824687	09117/824686
empirical formula, fw (g/mol)	C ₈₆ H ₁₃₆ N ₆ Na ₂ Nb ₂ O ₂ P ₆ , 1703.700	C ₆₃ H ₁₀₈ N ₃ NaNbO ₆ P ₅ , 1274.332
cryst size (mm ³)	0.25 × 0.10 × 0.10	0.60 × 0.35 × 0.20
temperature (K)	100(2)	100(2)
wavelength (Å)	0.710 73	0.710 73
cryst syst, space group	monoclinic, P2 ₁ /n	monoclinic, Cc
unit cell dimens (Å, deg)	a = 12.8900(9), α = 90 b = 19.0324(14), β = 100.1870(10) c = 19.1027(14), γ = 90	a = 45.936(4), α = 90 b = 12.7624(10), β = 107.7930(10) c = 25.324(2), γ = 90
volume (Å ³)	4612.5(6)	14136.0(19)
Z	2	8
density (calcd, g/cm ³)	1.227	1.198
abs coeff (mm ⁻¹)	0.408	0.336
F(000)	1808	5456
θ range for data collection (deg)	1.52–29.58	0.93–26.37
index ranges	−17 ≤ h ≤ 17, −26 ≤ k ≤ 26, −26 ≤ l ≤ 26	−57 ≤ h ≤ 57, −15 ≤ k ≤ 15, −31 ≤ l ≤ 31
reflns collected	119 506	118 612
indep reflns (R _{int})	12 950 (0.0630)	28 903 (0.0484)
completeness to θ _{max} (%)	100.0	100.0
max and min transmn	0.9603 and 0.9049	0.9358 and 0.8237
data/restraints/param	12 950/0/484	28 903/5058/1783
GOF ^d	1.046	1.031
final R indices ^b [I > 2σ(I)]	R ₁ = 0.0335, wR ₂ = 0.0748	R ₁ = 0.0403, wR ₂ = 0.0874
R indices ^b (all data)	R ₁ = 0.0540, wR ₂ = 0.0842	R ₁ = 0.0579, wR ₂ = 0.0969
largest diff peak and hole (e/Å ³)	0.463 and 0.660	0.521 and 0.752

^a GOF = {Σ[w(F_o² − F_c²)]/(n − p)}^{1/2}. ^b R₁ = (Σ||F_o − |F_c||)/Σ|F_o|; wR₂ = {Σ[w(F_o² − F_c²)]/Σ[w(F_o²)]}^{1/2}; w = 1/[σ²(F_o²) + (aP)² + bP]; P = [2F_c² + max(F_o², 0)]/3.

²J_{cd} = −34 Hz), −59.3 (t, P^d, ¹J_{de} = 351 Hz), −86.8 (t, P^e). ¹³C{¹H} NMR (C₆D₆, 20 °C, 125.8 MHz): δ 158.6 (*i*-Ar^{Nb}), 153.9 (*i*-Ar^{Nb}), 153.1 (*i*-Ar^P), 138.6 (*m*-Ar^{Nb}), 138.4 (*m*-Ar^{Nb}), 138.2 (*m*-Ar^P), 125.0 (*p*-Ar^{Nb}), 123.2 (*p*-Ar^{Nb}), 122.7 (*o*-Ar^{Nb}), 122.6 (*p*-Ar^P), 120.5 (*o*-Ar^{Nb}), 119.4 (*o*-Ar^P), 76.4 (CH₂^{Nb}), 70.5 (CH₂^{Nb}), 67.1 (CH₂^P), 38.6 (C(CH₃)₃^{Nb}), 36.5 (C(CH₃)₃^{Nb}), 36.2 (C(CH₃)₃^P), 31.0 (C(CH₃)₃^{Nb}), 29.9 (C(CH₃)₃^{Nb}), 29.4 (C(CH₃)₃^P), 22.5 (Ar^P-CH₃), 22.1 (Ar^{Nb}-CH₃). Combustion analysis was not obtained because of repeated and non-stoichiometric desolvation of etherate.

5.6. Product Distribution versus Solvent from the Activation of P₄ with Phosphide 1. Solid P₄ (13 mg, 0.10 mmol, 2.7 equiv) was added in excess to a solution of phosphide [Na(OEt₂)]₂[1] (30 mg, 0.038 mmol, 1.0 equiv), and the mixture was allowed to stir for 1 h before the product mixture was analyzed by ³¹P NMR spectroscopy. The anilide-bound phosphorus signal (at ca. +80 ppm) of 3 was integrated versus the signal of 2 (at ca. −200 ppm). The relative product ratios in various solvents are summarized in Table 1.

5.7. Generation of AsP₃ from the Anion 2. [Na(OEt₂)]₂[(P₃)Nb(N[Np]Ar)₃]₂ (75 mg, 0.044 mmol, 0.5 equiv) was dissolved in 2 mL of THF and frozen in a glovebox cold-well. Upon thawing, AsCl₃ (16 mg, 0.088 mmol, 1.0 equiv) was added via a microsyringe under stirring. The reaction mixture was allowed to stir for 30 min, during which time the reaction mixture became heterogeneous. This was taken to dryness under reduced pressure, and the resulting residue was slurried in C₆D₆ and filtered through Celite pads. P₄ (4.6 mg, 0.037 mmol, 0.42 equiv) was added from a stock solution in C₆D₆ to be used as the internal standard for ³¹P NMR spectroscopy. The formation of only Cl₂Nb(N[Np]Ar)₃ was observed by ¹H NMR spectroscopy and AsP₃ by ³¹P NMR spectroscopy.

5.8. X-ray Crystallographic Studies. Diffraction-quality orange crystals of [Na(THF)]₂[2]₂ were grown from toluene at −35 °C after the sample had been exposed to THF. Red crystals of [Na(THF)₆][3] were grown from a THF–pentane mixture at −35 °C. The crystals were mounted in hydrocarbon oil on a nylon loop or a glass fiber. Low-temperature (100 K) data were collected on a Siemens Platform three-circle diffractometer coupled to a Bruker-AXS Smart Apex CCD detector with graphite-monochromated Mo Kα radiation (λ = 0.710 73 Å) performing φ and ω scans. A semiempirical absorption correction was applied to the diffraction data using SADABS.³⁰ Both structures were solved by direct or Patterson methods using SHELXS^{31,32} and refined against F² on all data by full-matrix least squares with SHELXL-97.^{32,33} All non-hydrogen atoms were refined anisotropically. All hydrogen atoms were included in the model at geometrically calculated positions and refined using a riding model. The isotropic displacement parameters of all hydrogen atoms were fixed to 1.2 times the U_{eq} value of the atoms they are linked to (1.5 times for methyl groups).

No uncoordinated solvent molecules and no disorders were observed for the structure of [Na(THF)]₂[2]₂. For [Na(THF)₆][3], refinement was initially attempted in the C2/c space group, which yielded an unsatisfactory solution with large disorders, especially for the phosphorus-bound anilide ligand. The structure refined with fewer disorders as a racemic twin in the Cc space group, with two inequivalent molecules per asymmetric unit. The disorder in 10 of the 12 THF rings was refined within SHELXL with the help of rigid bond restraints as well as similarity restraints on the anisotropic displacement parameters for neighboring atoms and on 1,2 and 1,3 distances throughout the disordered components.³⁴ The relative occupancies of disordered components were refined freely within SHELXL. Further details are provided in Table 2 and in the form of CIF files available from the CCDC.³⁵

5.9. Computational Studies. All DFT calculations were carried out using the ORCA2.8 quantum chemistry program package from the development team at the University of Bonn.²⁹ In all cases, the local-density approximation functional employed was that of Perdew (PW-LDA),³⁶ while the generalized gradient approximation part was handled using the functionals of Becke and Perdew (BP86).³⁷ In addition, all calculations were carried out using the zero-order regular approximation (ZORA),³⁸ in conjunction with the SARC-TZV(2pf) basis set for niobium, the SARC-TZV basis set for hydrogen, and the SARC-TZV(p) set for all other atoms.³⁹ Spin-restricted Kohn–Sham determinants have been chosen to describe the closed-shell wave functions, employing the RI approximation and the tight self-consistent-field convergence criteria provided by ORCA. All calculations were reoptimized using the COSMO solvation model, as implemented in ORCA, set for either the dielectric constant of toluene or that of THF.⁴⁰

All structures were derived from the reported crystal structures by truncating the anilide ligand to NMePh. Plausible intermediate structures were derived from the optimized structure of $[\text{PNb}(\text{NMePh})_3]^-$ by building likely intermediates and allowing them to optimize with looser convergence criteria and using an economical basis set: SV for nonmetals and TZV(p) for niobium. Single-point calculations were run to determine the final energies with the following basis sets: TZV(2pf) for niobium, TZV(p) for hydrogen, and TZV(2d) for all other atoms. The coordinates of the optimized structures for the three anions, the three intermediates P₂, and P₄ are provided in the Supporting Information.

■ ASSOCIATED CONTENT

Supporting Information. Crystallographic data in CIF format, additional spectroscopic details of the reported products, as well as details on the stoichiometry of the P₄ activation with $[\text{Na}(\text{OEt}_2)]_2[1]_2$, on the activation of P₄ with $[\text{Na}(12\text{-crown-4})_2]^-$, $[(\text{P}_3)\text{Nb}(\text{N}[\text{Np}]\text{Ar})_3]$ and $[\text{Na}(\text{OEt}_2)][\text{As}=\text{Nb}(\text{N}[\text{Np}]\text{Ar})_3]$, on the activation of AsP₃ with $[\text{Na}(\text{OEt}_2)]_2[1]_2$, and on attempts to intercept P₂ with dienes, together with coordinates for the computed structures. This material is available free of charge via the Internet at <http://pubs.acs.org>.

■ AUTHOR INFORMATION

Corresponding Author

*E-mail: ccummins@mit.edu.

■ ACKNOWLEDGMENT

This material is based upon work supported by the National Science Foundation under Grants CHE-0719157 and CHE-1111357. For support, including a gift of white phosphorus, we thank Thermphos International. We thank Dr. Anthony F. Cozzolino and Dr. Nicholas A. Piro for assistance with computations and crystallography, respectively.

■ REFERENCES

- (1) Di Vaira, M.; Ghilardi, C. A.; Midollini, S.; Sacconi, L. *J. Am. Chem. Soc.* **1978**, *100*, 2550–2551.
- (2) Caporali, M.; Gonsalvi, L.; Rossin, A.; Peruzzini, M. *Chem. Rev.* **2010**, *110*, 4178–4235.
- (3) Cossairt, B. M.; Piro, N. A.; Cummins, C. C. *Chem. Rev.* **2010**, *110*, 4164–4177.
- (4) Hoffmann, R. *Angew. Chem., Int. Ed. Engl.* **1982**, *21*, 711–724.
- (5) Piro, N. A.; Cummins, C. C. *J. Am. Chem. Soc.* **2008**, *130*, 9524–9535.
- (6) Piro, N. A.; Figueroa, J. S.; McKellar, J. T.; Cummins, C. C. *Science* **2006**, *313*, 1276–1279.

- (7) Cossairt, B. M.; Diawara, M.-C.; Cummins, C. C. *Science* **2009**, *323*, 602.
- (8) Scheer, M.; Balázs, G.; Seitz, A. *Chem. Rev.* **2010**, *110*, 4236–4256.
- (9) Figueroa, J. S.; Cummins, C. C. *Angew. Chem., Int. Ed.* **2004**, *43*, 984–988.
- (10) Spek, A. L. *Acta Crystallogr.* **2009**, *D65*, 148–155.
- (11) Budzelaar, P. H. M. *gNMR, NMR Simulation Program*, version 5.0.6.0; Ivory Software Corp.: Centennial, CO, 2006.
- (12) Spinney, H. A.; Piro, N. A.; Cummins, C. C. *J. Am. Chem. Soc.* **2009**, *131*, 16233–16243.
- (13) Cambridge Structural Database deposition numbers 824686 and 824687, The Cambridge Crystallographic Data Centre, Cambridge, U.K.
- (14) Hirsekorn, K. F.; Veige, A. S.; Wolczanski, P. T. *J. Am. Chem. Soc.* **2006**, *128*, 2192–2193.
- (15) Baudler, M.; Glinka, K. *Chem. Rev.* **1993**, *93*, 1623–1667.
- (16) (a) Wanandi, P. W.; Davis, W. M.; Cummins, C. C.; Russell, M. A.; Wilcox, D. E. *J. Am. Chem. Soc.* **1995**, *117*, 2110–2111. (b) Rупpa, K. B. P.; Desmangles, N.; Gambarotta, S.; Yap, G.; Rheingold, A. L. *Inorg. Chem.* **1997**, *36*, 1194–1197.
- (17) Cotton, F. A.; LaPrade, M. D. *J. Am. Chem. Soc.* **1968**, *90*, 5418–5422.
- (18) Urnius, E.; Brennessel, W. W.; Cramer, C. J.; Ellis, J. E.; von Ragué Schleyer, P. *Science* **2002**, *295*, 832–834.
- (19) (a) Gumsheimer, U. Reactions of Complexes of the Type $[\text{Cp}^R\text{M}(\text{CO})_3\text{X}]$ (M = Mo, W; X = Me, H) with $[\text{Cp}^R\text{Fe}(\eta^5\text{-P}_5)]$ and White Phosphorus. Ph.D. Thesis, Universität Kaiserslautern, Kaiserslautern, Germany, 2002; (b) Peruzzini, M.; Abdreimova, R. R.; Budnikova, Y.; Romerosa, A.; Scherer, O. J.; Sitzmann, H. *J. Organomet. Chem.* **2004**, *689*, 4319–4331.
- (20) Detzel, M.; Mohr, T.; Scherer, O. J.; Wolmershäuser, G. *Angew. Chem., Int. Ed.* **1994**, *33*, 1110–1112.
- (21) (a) Scherer, O. J.; Hübel, B.; Wolmershäuser, G. *Angew. Chem., Int. Ed.* **1992**, *31*, 1027–1028. (b) Scherer, O. J.; Berg, G.; Wolmershäuser, G. *Chem. Ber.* **1996**, *129*, 53–58. (c) Scherer, O. J.; Vömecke, T.; Wolmershäuser, G. *Eur. J. Inorg. Chem.* **1999**, *1999*, 945–949.
- (22) Ceccconi, F.; Ghilardi, C. A.; Midollini, S.; Orlandini, A. *J. Am. Chem. Soc.* **1984**, *106*, 3667–3668.
- (23) Cossairt, B. M.; Cummins, C. C. *J. Am. Chem. Soc.* **2009**, *131*, 15501–15511.
- (24) (a) Wohlfarth, C. Permittivity (Dielectric Constant) of Liquids. In *CRC Handbook of Chemistry and Physics*, 91st ed.; Haynes, W. M., Ed.; CRC Press: Boca Raton, FL, 2010–2011; pp 187–207; (b) Drain, C. M.; Gentemann, S.; Roberts, J. A.; Nelson, N. Y.; Medforth, C. J.; Jia, S.; Simpson, M. C.; Smith, K. M.; Fajer, J.; Shelnut, J. A.; Holten, D. *J. Am. Chem. Soc.* **1998**, *120*, 3781–3791.
- (25) Galiano-Roth, A. S.; Collum, D. B. *J. Am. Chem. Soc.* **1989**, *111*, 6772–6778.
- (26) Tofan, D.; Cummins, C. C. *Angew. Chem., Int. Ed.* **2010**, *49*, 7516–7518.
- (27) Esterhuysen, C.; Frenking, G. *Chem.—Eur. J.* **2003**, *9*, 3518–3529.
- (28) Koch, W.; Holthausen, M. C. *A Chemist's Guide to Density Functional Theory*, 2nd ed.; Wiley-VCH: New York, 2001.
- (29) Neese, F. *ORCA—an ab initio, Density Functional and Semiempirical program package*, version 2.8.0; University of Bonn: Bonn, Germany, 2009.
- (30) Sheldrick, G. M. *SHELXTL*; Bruker AXS, Inc.: Madison, WI, 2005–2011.
- (31) Sheldrick, G. M. *Acta Crystallogr., Sect. A: Fundam. Crystallogr.* **1990**, *46*, 467–473.
- (32) Sheldrick, G. M. *Acta Crystallogr., Sect. A* **2008**, *64*, 112–122.
- (33) Sheldrick, G. M. *SHELXL-97: Program for crystal structure determination*; University of Göttingen: Göttingen, Germany, 1997.
- (34) Müller, P.; Herbst-Irmer, R.; Spek, A. L.; Schneider, T. R.; Sawaya, M. R. In *Crystal Structure Refinement: A Crystallographer's Guide to SHELXL*; Müller, P., Ed.; IUCr Texts on Crystallography; Oxford University Press: Oxford, U.K., 2006.

(35) These data can be obtained free of charge from The Cambridge Crystallographic Data Centre via http://www.ccdc.cam.ac.uk/data_request/cif.

(36) Perdew, J. P.; Wang, Y. *Phys. Rev. B: Condens. Matter* **1992**, *45*, 13244–13249.

(37) (a) Becke, A. D. *Phys. Rev. A* **1988**, *38*, 3098–3100. (b) Perdew, J. P. *Phys. Rev. B: Condens. Matter* **1986**, *33*, 8822–8824.

(38) (a) Lenthe, E.; Baerends, E. J.; Snijders, J. G. *J. Chem. Phys.* **1993**, *99*, 4597–4610. (b) Heully, J. L.; Lindgren, I.; Lindroth, E.; Lundqvist, S.; Maartensson-Pendrill, A. M. *J. Phys. B: At. Mol. Phys.* **1986**, *19*, 2799–2815.

(39) Schaefer, A.; Horn, H.; Ahlrichs, R. *J. Chem. Phys.* **1992**, *97*, 2571–2577.

(40) Sinnecker, S.; Rajendran, A.; Klamt, A.; Diedenhofen, M.; Neese, F. *J. Phys. Chem. A* **2006**, *110*, 2235–2245.